

4-(*tert*-butyl)-*N,N*-diethylbenzenesulfonamide: Structural, absorption distribution metabolism excretion toxicity (ADMET) and molecular docking studies

Gurumallappa^a, Jayashankar Jayaprakash^a, Ananda A. Puttaswamy^b, Jayanth H. Sunderraj^{*c},
Puttaswamappa Mallu^a and Krishnamurthy N. Beeregowda^d

^aDepartment of Chemistry, SJCE, JSS Science and Technology University, Mysuru-570 006, Karnataka, India

^bGanesh Consultancy and Analytical Services, Hebbal Industrial Area, Mysuru-570016, Karnataka, India

^cDepartment of Microbiology, Yuvaraja's College, University of Mysore, Manasagangotri, Mysuru-570005, Karnataka, India

^dResearch and Development Centre, Bharathiyar University, Coimbatore, Tamil Nadu-641046, India

CHRONICLE

Article history:

Received November 18, 2020

Received in revised form

March 22, 2021

Accepted March 22, 2021

Available online

March 22, 2021

Keywords:

Antibacterial agent

ADMET

DNA gyrase

Molecular docking

Sulfonamide

ABSTRACT

Sulfonamides are a very good antibacterial agent that targets essential bacterial enzymes specifically DNA gyrase. The objective of the present work was to investigate the molecular docking of the (4-(*tert*-butyl)-*N,N*-diethylbenzenesulfonamide) with the DNA gyrase of *S. aureus*. The energy-free topoisomerase activity of the A subunit, which breaks the DNA, is inhibited by 4-quinolones such as nalidixic acid and ciprofloxacin. The energy transducing activity of the B subunit is inhibited by novobiocin and other coumarin antibiotics. Single crystal X-ray diffractometer study was carried out to understand the structure, physical and chemical reactive parameters, the title compound is crystallized under monoclinic crystal system with the space group of P21/C. To understand the behaviour of the title compound in living organism, Absorption, Distribution, Metabolism, Excretion analysis was done using Swiss ADME and Osiris data warrior tool. Further, Toxicity of the title compound was predicted by using PKCSM online software.

© 2021 Growing Science Ltd. All rights reserved.

1. Introduction

Bacterial infections are important from the point of public health and are easier to treat than viral infections. There are a variety of methods, antibiotics and drugs available in treating bacterial infections.¹ In the current days, bacterial resistance to antimicrobials is a growing problem. Microorganisms have developed resistance to antibiotics and drugs naturally in the due course of time due to indiscriminate and inappropriate use of antimicrobials. This natural adaptation phenomenon has become the principal problem worldwide for the treatment of infectious diseases. This has also created a continuous need for the discovery of new chemical entities with antibiotic properties.²⁻⁴ The new chemical entities should show broad spectrum activity and to be safe for use.

* Corresponding author.

E-mail address: drmallu66@gmail.com (J. H. Sunderraj)

The present study provides insight into the use of (4-(*tert*-butyl)-*N,N*-diethylbenzenesulfonamide) as an antimicrobial substance as shown in **Fig. 1**. Sulfa drugs have been widely used to treat a broad spectrum of microbial diseases. The sulphonamide group is present in many of the biologically active molecules which are used as antimicrobial agents. A number of sulphonamide derivatives shows anticancer and anti-inflammatory activities.⁵ There is great insight to search for potent pharmacologically active sulphonamide and its derivatives.⁶⁻⁸ In this present study, single crystal X-ray diffractometer was studied to confirm the molecular structure, interactions and packing diagram and mainly deals on molecular docking and ADMET studies of 4-(*tert*-butyl)-*N,N*-diethylbenzenesulfonamide with DNA gyrase.

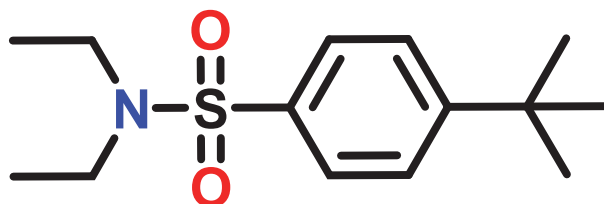


Fig. 1. Structure of 4-(*tert*-butyl)-*N,N*- diethylbenzenesulfonamide

2. Results and Discussion

2.1 Crystal structure analysis

The structure of the title compound was determined by single crystal X-ray diffraction studies. The compound crystallizes in the monoclinic space group $P2_1/c$. The X-ray analysis revealed that the crystal structure of title compound is highly nonplanar **Fig. 2**. The molecular packing diagram of title compound along a-axis and b-axis are shown in **Fig. 3 and Fig. 4**. The selected bond lengths, bond angles and torsion angles are listed in the **Table 1, 2 and 3**.

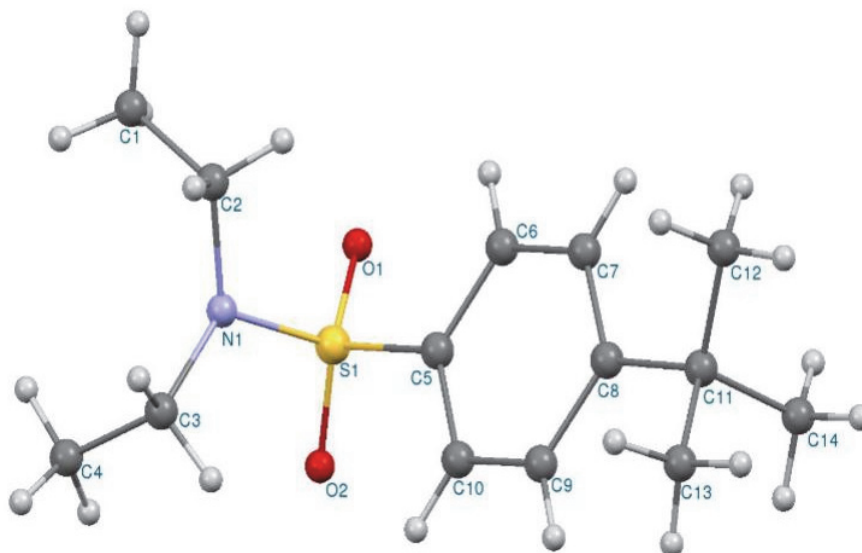


Fig. 2. Crystal structure of the title compound with atom numbering.

Table 1. Selected bond lengths of title compound (°)

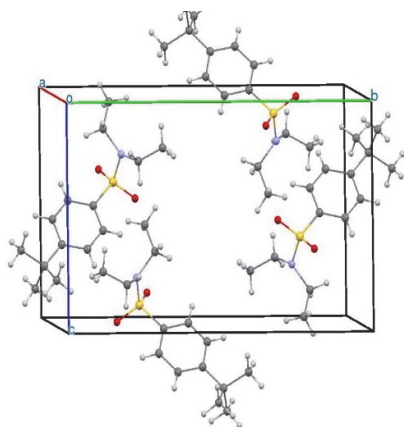
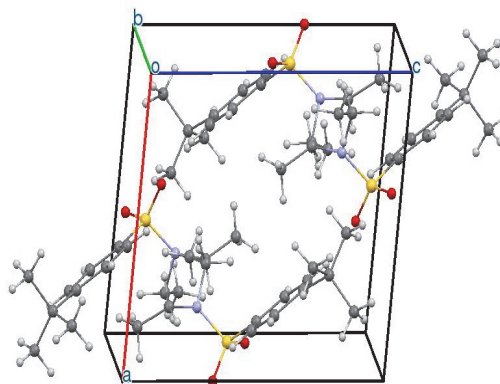
Atoms	Length	Atoms	Length
S1-O1	1.418(4)	C5-C10	1.390(7)
S1-O2	1.422(5)	C6-C7	1.385(6)
S1-N1	1.597(5)	C7-C8	1.391(5)
S1-C5	1.763(5)	C8-C9	1.412(6)
N1-C2	1.507(9)	C8-C11	1.524(7)
N1-C3	1.509(9)	C9-C10	1.374(7)
C1-C2	1.437(10)	C11-C12	1.491(12)
C3-C4	1.447(12)	C11-C13	1.517(9)
C5-C6	1.400(6)	C11-C14	1.499(11)

Table 2. Selected bond angles of title compound (°).

Atoms	Length	Atoms	Length
S1-O1	1.418(4)	C5-C10	1.390(7)
S1-O2	1.422(5)	C6-C7	1.385(6)
S1-N1	1.597(5)	C7-C8	1.391(5)
S1-C5	1.763(5)	C8-C9	1.412(6)
N1-C2	1.507(9)	C8-C11	1.524(7)
N1-C3	1.509(9)	C9-C10	1.374(7)
C1-C2	1.437(10)	C11-C12	1.491(12)
C3-C4	1.447(12)	C11-C13	1.517(9)
C5-C6	1.400(6)	C11-C14	1.499(11)

Table 3. Torsion angles of title compound (°)

Atoms	Angle	Atoms	Angle
O1-S1-N1-C2	-46.6(5)	S1-C5-C6-C7	-179.7(3)
O1-S1-N1-C3	165.7(5)	C10-C5-C6-C7	-0.3(6)
O2-S1-N1-C2	-175.9(4)	S1-C5-C10-C9	178.8(3)
O2-S1-N1-C3	36.4(5)	C6-C5-C10-C9	-0.5(6)
C5-S1-N1-C2	68.2(5)	C5-C6-C7-C8	1.1(7)
C5-S1-N1-C3	-79.5(5)	C6-C7-C8-C9	-0.9(6)
O1-S1-C5-C6	21.4(4)	C6-C7-C8-C11	176.8(4)
O1-S1-C5-C10	-157.9(4)	C7-C8-C9-C10	0.1(6)
O2-S1-C5-C6	151.6(4)	C11-C8-C9-C10	-177.6(4)
O2-S1-C5-C10	-27.8(4)	C7-C8-C11-C12	31.0(7)
N1-S1-C5-C6	-93.2(4)	C7-C8-C11-C13	152.0(5)
N1-S1-C5-C10	87.4(4)	C7-C8-C11-C14	-93.0(6)
S1-N1-C2-C1	113.6(6)	C9-C8-C11-C12	-151.4(6)
C3-N1-C2-C1	-97.8(7)	C9-C8-C11-C13	-30.4(7)
S1-N1-C3-C4	-103.5(7)	C9-C8-C11-C14	84.6(6)
C2-N1-C3-C4	108.4(7)	C8-C9-C10-C5	0.6(7)

**Fig. 3.** Molecular packing of title compound along *a*-axis**Fig. 4.** Molecular packing of title compound along *b*-axis

2.2 Molecular docking studies

DNA gyrase protein is an enzyme that controls replication of DNA by regulating negative supercoiling of bacterial DNA. The inhibition of subunit (Gyrase A) of protein, influences the metabolic pathways by breaking and rejoining the DNA. This protein is an important target to discover various drugs, and could be useful to overcome from multidrug resistant problems. In this study, the title compound and sulfamethoxazole which is used as a standard drug is docked (*in-silico* computer-aided) with the DNA gyrase protein. Exploration on ligand-protein interactions and binding orientations gives a good understanding about the binding site of the targeted DNA gyrase protein of *S. aureus*. Lower the binding free energy indicates the stronger binding affinity between the protein and ligands, emphasizing the binding modes of title compound and standard drug with DNA gyrase protein. **Fig. 5** shows the interaction type of the title compound, revealing binding affinity towards protein with a binding score -6.6 kcal/mol. Title compound interacts with the DGE5 and PHE1097 amino acids. Whereas **Fig. 6** showing the interaction of standard drug (sulfamethoxazole), shows good binding affinity towards protein with a score -7.6 kcal/mol. Standard drugs interact with the SER1098, ARG1092, VAL1091, PHE1097 and VAL1268 amino acids. The detailed interactions in the binding process (Bond length and docking energies) are given in **Table 4**.

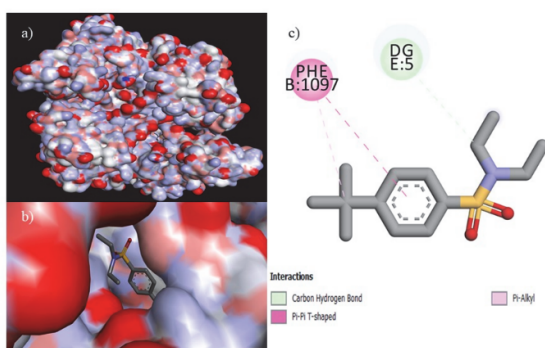


Fig. 5. Molecular docking of Title compound with 6FM4. (a) Docking surface pocket pose, (b) docking interaction at surface, (c) 2D protein-ligand interaction

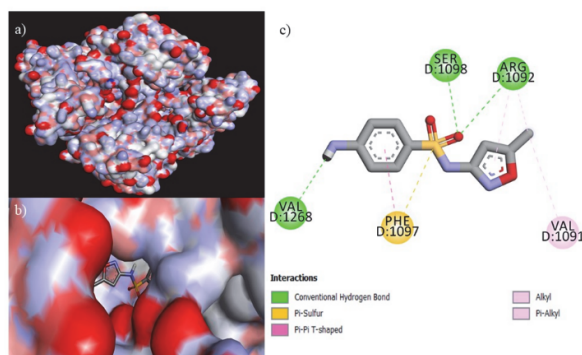


Fig. 6. Molecular docking of Sulfamethoxazole with 6FM4. (a) Docking surface pocket pose, (b) docking interaction at surface, (c) 2D protein-ligand interaction

Table 4. Interaction between ligands and 6M0J viral protein

PDB ID	Compound	Protein	Ligand	Interaction type	Distance	binding
6FM4	Title compound	DGE5	Carbon	Carbon	3.50	-6.6
		PHE1097	Carbon	π - Alkyl	5.10	
		PHE1097	π of Benzene	π - π - T-Shaped	5.15	
	Sulfamethoxazole	VAL1268	Hydrogen	Conventional	2.27	-7.6
		SER1098	Oxygen	Conventional	2.34	
		ARG1092	Oxygen	Conventional	3.02	
		ARG1092	Carbon	Alkyl	4.33	
		PHE1097	π of Benzene	π - π - T - Shaped	4.84	
		VAL1091	Carbon	Alkyl	5.03	
		ARG1092	π of Isoxazole	π - Alkyl	5.43	
		PHE1097	π of Sulfur	π - Sulfur	5.68	

2.3 ADME and Toxicity Prediction

Many chemical entities may not be used as drugs finally due to the poor pharmacokinetics and unfavorable toxicity properties in the drug development process. *In silico* ADMET study is the best method to identify those results. By using a Swiss ADME and pkCSM online tool we can determine ADMET properties and drug likeness of the title compound and sulfamethoxazole which is used as a standard drug for the comparison. The physiochemical properties of the (4-(*tert*-butyl)-*N,N*-

diethylbenzenesulfonamide) and sulfamethoxazole were calculated by using Osiris datawarrior and depicted in the **Table 5**.

Table 5. Physicochemical parameters generated using Osiris datawarrior

Property Name	Property Value
Molecular Weight	269.40 g/mol
Clog P	3.2727
Clog S	-2.515
Hydrogen Bond Donor Count	0
Hydrogen Bond Acceptor Count	3
Rotatable Bond Count	4
TSA	211.37
RPSA	0.15201
PSA	45.76 Å
Shape Index	0.55556
Molecular Flexibility	0.66498
Molecular Complexity	0.63466
Stereo Centers	0
Druglikness	-0.81078

The BOILED-Egg model and bioavailability radar of the title compound (Molecule 1) and standard drug (Molecule 2) are shown in **Fig. 7**. The compound shows a good bioavailability score (0.55%) and includes all the parameters such as XLOGP3=3.48, Molecular weight=260.40 g/mol, POLAR = 45.76 Å², Solubility (Log S) = -3.62, Flexibility (FLEX) = 5, (INSATU) = 0.57 which lie within the acceptable range. The ADMET results are interpreted as title compound shows a good gastrointestinal absorption (95%) than standard compound (76%). The title compound has low skin permeability whereas standard drug has high skin permeability (logKp>-2.5). The volume of distribution (VDss) of a standard drug shows a low value of LogVDss whereas our compound gives the moderate value of LogVDss and both the compounds readily cross the Blood Brain Barrier (BBB) and are considered to penetrate the central nervous system. Whether the title compound and standard drug are likely to be a cytochrome P450 inhibitor or it is metabolized by P450 substrate has also been investigated and possibility of the given compound is likely to be OCT2 substrate has also been given and depicted in **Table 6**. The prediction of the toxicity is important for the drug development system. In this method, it is important to predict whether a given compound is toxic in nature or not and the techniques consumes less time and is rapid. The 0.883 log mg/kg/day and 0.734 log mg/kg/day has been found to be the maximum tolerated dose for the human in compound and standard drug one and 2.289mol/kg and 1.835log mg/kg_{bw}/day the oral rat acute and chronic toxicity of the title compound. The results indicate that the compound is less toxic in nature (**Table 6**). From all the methods such as Lipinski, Ghose, Veber, Egen and Muegge the compound shows a Drug likeness property.

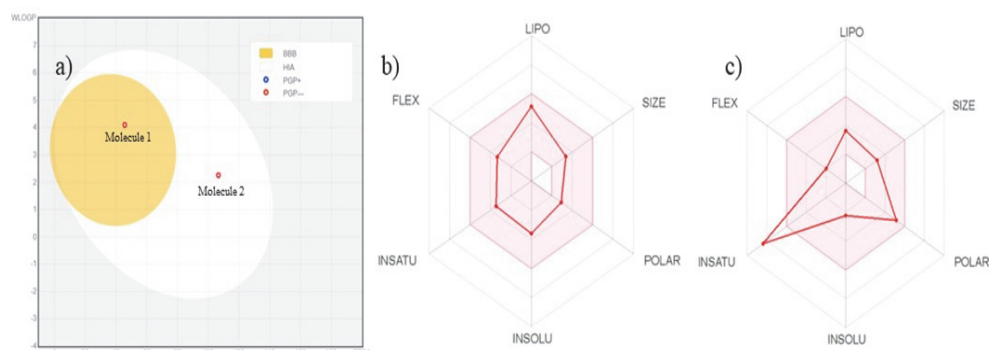


Fig. 7. (a) The BOILED-Egg model, (b) Bioavailability radar of title compound and (c) Bioavailability radar of standard drug

Table 6. ADME and Toxicity by using pkCSM tool

Parameters		Predicted Value	
		Title compound	Sulfamethoxazole
Absorption	Water solubility (log mol/L)	-4.219	-2.237
	Caco2 permeability (log Papp in 10 ⁻⁶ cm/s)	1.034	0.039
	Intestinal absorption (human) (% Absorbed)	95.063	76.705
	Skin Permeability (log Kp)	-2.414	-2.916
	P-glycoprotein substrate	No	No
	P-glycoprotein I inhibitor	No	No
	P-glycoprotein II inhibitor	No	No
Distribution	VDss (human) (log L/kg)	0.115	-0.235
	Fraction unbound (human) (Fu)	0.062	0.37
	BBB permeability (log BB)	0.291	-0.566
	CNS permeability (log PS)	-1.954	-2.993
Metabolism	CYP2D6 substrate	No	No
	CYP3A4 substrate	Yes	No
	CYP1A2 inhibitor	Yes	No
	CYP2C19 inhibitor	Yes	No
	CYP2C9 inhibitor	No	No
	CYP2D6 inhibitor	No	No
	CYP3A4 inhibitor	No	No
Excretion	Total Clearance (log ml/min/kg)	1.571	0.412
	Renal OCT2 substrate	No	No
Toxicity	AMES toxicity	No	No
	Max. tolerated dose (human) (log mg/kg/day)	0.883	0.734
	hERG I inhibitor	No	No
	hERG II inhibitor	No	No
	Oral Rat Acute Toxicity (LD50) (mol/kg)	2.289	2.008
	Oral Rat Chronic Toxicity (LOAEL) (log mg/kg_bw/day)	1.835	1.226
	Hepatotoxicity	No	Yes
	Skin Sensitisation	No	No
	T. Pyriformis toxicity (log ug/L)	1.147	0.402
Minnnow toxicity (log mM)	0.325	2.116	

3. Conclusion

In this present investigation, deliberated the structural properties of the title compound and validate them with theoretical results such as molecular docking and ADMET studies. X-ray structural evaluation of (4-(tert-butyl)-*N,N*-diethylbenzenesulfonamide) exposed that the intermolecular interactions such as conventional hydrogen bond, short interactions, and C-H bond greatly contributes to the ligand-protein binding process. The *in-silico* molecular docking studies clearly explain that the compound interacted well with a target protein and reveals the information about protein-ligand interaction and binding affinity title compound was seen to be -6.6 kcal/mol and standard drug -7.6 kcal/mol with DNA *gyrase* protein. ADMET prediction were also discussed for the title compound and it shows that the maximum tolerated dose for a human is 0.883 Log mg/Kg/day in addition chronic toxicity is 1.835 Log mg/kg_bw/day this indicating that the compound (4-(tert-butyl)-*N,N*-diethylbenzenesulfonamide) is less toxic. This investigation will be helpful for further studies about the design and synthesis of new antibacterial compounds in the future.

4. Experimental

4.1. Materials

The compound (4-(tert-butyl)-*N,N*-diethylbenzenesulfonamide) was purchased from Sigma-Aldrich. All necessary solvents used for the crystallization were purchased from Merck Pvt.Ltd and SD fine chemicals and used without further purification.

4.2. Crystal Growth

The title compound was dissolved in suitable organic solvents like ethanol, methanol and dichloromethane. The formation of single crystals was observed after a week in dichloromethane solution. The suitable crystals were taken, dried and subjected for further studies.

4.3. X-ray diffraction studies

Single crystal of the title compound was selected for the data collection. Single crystal X-ray intensity data were collected at 293 K using graphite-monochromate Mo-K α ($\lambda=0.71073$ Å) radiation equipped with Rigaku XtaLAB mini three-circle CCD diffractometer. The data collection strategy was planned and executed using *CrystalClear-SM Expert 2*.⁹ The structure solution was carried out using direct methods and refinement was done by full-matrix least-squares against F^2 using *SHELXS* and *SHELXL-2018*.^{10,11} Crystal structure geometry calculations were carried out using the *PLATON* program.¹² The ORTEP and packing diagrams of the title compound were generated using *MERCURY 4.2.0*.¹³ The complete crystallographic data and refinement parameters of the title compound are summarized in **Table 7**.

Table 7. Crystal structure data and refinement details of the title compound.

Empirical formula	C ₁₄ H ₂₃ NO ₂ S	Reflections collected	8919
Formula weight	269.39	Independent reflections	3501 [R _{int} = 0.1767]
Temperature (K)	293 K	Refinement method	Full matrix least-
Wavelength (Å)	0.71075	Data/restraints/parameters	3501 / 0 / 168
Crystal system, space group	<i>Monoclinic, P2₁/n</i>	Goodness-of-fit on F^2	1.071
Unit cell dimensions		Final [$I > 2\sigma(I)$]	$RI = 0.1053$, $wR2 =$
Z	4	R indices (all data)	$RI = 0.1925$, $wR2 =$
Density (calculated) in (Mg m ⁻³)	1.126	a (Å)	9.476(8)
Absorption coefficient (mm ⁻¹)	0.199	b (Å)	16.50(3)
F_{000}	584	c (Å)	10.24(2)
θ range for data collection (°)	3.03 to 27.44	β (°)	96.75(3)
		Volume Å ³	1590(5)
Index ranges	$-12 \leq h \leq 11$	$-21 \leq k \leq 19$	$-12 \leq l \leq 13$

4.4. Molecular docking

In silico molecular docking study of title compound with DNA gyrase protein of *S. aureus* was carried out using MGL tools 1.5.6 with *AutoDock Vina*.¹⁴ The three-dimensional structures of *S. aureus* gyrase complex with ID-130 and DNA residues (PDB ID: 6FM4) was downloaded from the Protein Data Bank in PDB format. Inbound ligands were freed from the protein by Biovia Discovery Studio 2019 Client visualize.¹⁵ Using the AutoDock Tools (ADT) polar hydrogen atoms were added and energy minimized to the protein. The binding sites were defined using grid sizes of -34.59, 15.36, and 24.81 for X, Y, Z respectively. Through the command script provided by developers, the docking simulations were performed with *AutoDock Vina*. The binding affinity of novel ligands was observed as a negative score with the unit of kcal/mole. The obtained protein-ligand interactions were visualized and the binding sites were analyzed using Biovia Discovery Studio 2019 Client visualizer.

4.5. In silico ADMET and druglikeness prediction

The *In-silico* ADMET prediction (absorption, distribution, metabolism, excretion, toxicity) and druglikeness of the title compound were predicted using SwissADME and pkCSM online tool.¹⁶ The compound structure is drawn on Marvin JS software in 2-D structure format and those structures are imported into SMILES at the interface of the website (<http://swissadme.ch/>). The SMILES of those compounds was inserted into pkCSM online tool. The physicochemical properties of the title compound were calculated by using Osiris Datawarrior tool.¹⁷ The ADMET parameters include molecular weight, water solubility, drug likeness, PSA and BBB etc.¹⁸ By using pkCSM online tool the toxicity mode was selected and the toxicity effects such as AMES toxicity, human maximum tolerance dose, hepatotoxicity, skin toxicity and minnow toxicity.

References

1. Doron S., and Gorbach S.L. (2008) Bacterial infections: overview. International Encyclopedia of Public Health, Academic press 273-282.
2. De A.R.S.A., Barbosa F.J.M., Scotti M.T., Scotti L., Da Cruz R.M.D., Falco S.V.D.S., Siqueiera J. J.P.D., and Mendona J.F.J.B., (2016). Modulation of drug resistance in *Staphylococcus aureus* with Coumarin derivatives. *Scientifica.*, 1-6.
3. French G.L., (2010)., The continuing crisis in antibiotic resistance. *Int. J. of Antimicrobial agents.*, 36 S3-S7.
4. Jordheim L. P., Larbi S. B., Fendrich O., Ducrot C., Bergeron E., Dumonetet C., Freney J., and Doleans J. A., (2012). Gemcitabine is active against clinical multiresistant *Staphylococcus aureus* strains and is synergistic with gentamicin. *Int.J. of Antimicrobial agents.*, 39 444-447
5. Alsughayer A., Elassar A. Z. A., Mustafa S. and Al S. F., (2011). Synthesis, structure analysis and antibacterial activity of new potent sulfonamide derivatives. *J. Biomater. Nanobiotechnol.*, 2(02)143.
6. Wigley D. B., Davies G. J., Dodson E. J., Maxwell A., and Dodson G., (1991). Crystal structure of an N-terminal fragment of the DNA gyrase B protein. *Nature.*, 351(6328) 624-629.
7. Rigaku C. C. S., (2011). Expert 2.0 r15. *Software for Data Collection and Processing*. Rigaku Corporation, Tokyo, Japan.
8. Sheldrick G. M. (1990). Phase annealing in SHELX-90, direct methods for larger structures. *Acta Crystallogr, Sect.*, A46(6) 467-473.
9. Spek A. L., PLATON., (1990). An integrated tool for the analysis of the results of a single crystal structure determination. *Acta Crystallogr., Sect.*, A46(S1), C34-C34.
10. Marcrae C. F., Sovago I., Cottrell S. J., Galek P. T. A., McCabe P., Pidcock E., Platings M., Shields G. P., Stevens J. S., Towler M., and Wood P.A., (2020). Mercury 4.0: from visualization to analysis, design and prediction. *J. Appl. Crystallogr.*, 226-235.
11. Hema M. K., Renganathan R. A., Swamy S. N., Karthik C. S., Pampa K. J., Mallu P., Rai V. R., and Lokanath N. K., (2020). 4, 4, 4-Trifluoro-1-(thiophen-2-yl) butane-1, 3-dione nickel (II) complex: Synthesis, structure, quantum chemical and DNA binding studies. *J. Mol. Struct.*, 1202 127277.
12. Spek A. L., (2009). Structure validation in chemical crystallography. *Acta Crystallogr., Sect. D: Biol. Crystallogr.*, 65(2) 148-155.
13. Gupta A., Sharma V., Tewari A. K., Surender Kumar V., Wadhwa G., Mathur A., Sharma S.K., and Jain C. K., (2013). Comparative Molecular docking analysis of DNA gyrase subunit A in *Pseudomonas aeruginosa* PAO1. *J. Bioinform.*, 9(3) 116-120.
14. Zaki H., Belhassan A., Aouidate A., TaharLakhlifi A. A. T., Benlyas M., and Bouachrine M., (2019). Antibacterial study of 3-(2-amino-6-phenylpyrimidin-4-yl)-N-cyclopropyl-1-methyl-1H-indole-2-carboxamide derivatives: CoMFA, CoMSIA analyses, molecular docking and ADMET properties prediction. *J. Mol. Struct.*, 1177 275-285.
15. Islam M. A., and Pillay T. S., (2020). Identification of promising anti-DNA gyrase antibacterial compounds using de novo design, molecular docking and molecular dynamics studies. *J. Biomol. Struct.*, 38(6) 1798-1809.
16. Shinde M. G., Modi S. J., and Kulkarni V. M., (2017). Synthesis, pharmacological evaluation, molecular docking and in silico ADMET prediction of nitric oxide releasing biphenyls as anti-inflammatory agents. *J. Appl. Pharm. Sci.*, 7 37-47.
17. Matin M. M., Hasan M. S., Uzzaman M., Bhuiyan M. M. H., Kibria S. M., Hossain M. E., and Roshid M. H., (2020). Synthesis, spectroscopic characterization, molecular docking, and ADMET studies of mannopyranoside esters as antimicrobial agents. *J. Mol. Struct.*, 1222 128821.
18. Yadav K. D., Mudgal V., Agrawal J., Maurya K. A., Bawankule U. D., Chanotiya S. C., Khan F., and Thul T. S., (2013). Molecular docking and ADME studies of natural compounds of Agarwood oil for topical anti-inflammatory activity. *Curr Comput Aided Drug Des.*, 9(3) 360-370.

